HHS Public Access

Author manuscript

Leuk Lymphoma. Author manuscript; available in PMC 2015 April 06.

Published in final edited form as:

Leuk Lymphoma. 2014 August ; 55(8): 1876–1883. doi:10.3109/10428194.2013.862241.

Inhibition of type I insulin-like growth factor receptor tyrosine kinase by picropodophyllin induces apoptosis and cell cycle arrest in T lymphoblastic leukemia/lymphoma

Zhiwei Huang[1], **Zhijia Fang**[1], **Hong Zhen**[2], **Li Zhou**[2], **Hesham M. Amin**[3], and **Ping Shi**[2]

[1]College of Chemistry, Chemical Engineering and Biotechnology, Donghua University, Shanghai 201620, China

[2]State Key Laboratory of Bioreactor Engineering, East China University of Science and Technology, Shanghai 200237, China

[3]Department of Hematopathology, The University of Texas M. D. Anderson Cancer Center, Houston 77030, Texas, USA

Abstract

It has been recently shown that IGF-IR contributes significantly to the survival of T lymphoblastic leukemia/lymphoma (T-LBL) cells, and it was therefore suggested that IGF-IR could represent a legitimate therapeutic target in this aggressive disease. Picropodphyllin (PPP) is a potent, selective inhibitor of IGF-IR that is currently used with notable success in clinical trials that include patients with aggressive types of epithelial tumors. In the present study, we tested the effects of PPP on Jurkat and Molt-3 cells; two prototype T-LBL cell lines. Our results demonstrate that PPP efficiently induced apoptotic cell death and cell cycle arrest of these two cells. These effects were attributable to alterations of downstream target proteins. By using proteomic analysis, 7 different proteins were found to be affected by PPP treatment of Jurkat cells. These proteins are involved in various aspects of cellular metabolism, cytoskeleton organization, and signal transduction pathways. The results suggest that PPP affects multiple signaling molecules and inhibits fundamental pathways that control cell growth and survival. Our study also provides novel evidence that PPP could be potentially utilized for the treatment of the aggressive T-LBL.

Keywords

IGF-IR; T lymphoblastic leukemia/lymphoma; picropodophyllin; Jurkat cells; Molt-3 cells; proteomics

Address correspondence to: Ping Shi, Ph.D. Professor State Key Laboratory of Bioreactor Engineering East China University of Science and Technology No. 130 Meilong Roa Shanghai 200237, China Telephone: 011(86)-021-64251655 Fax: 011(86)-021064252920 ship@ecust.edu.cn Or Hesham M. Amin, M.D., M.Sc. Professor Department of Hematopathology, Unit 72 The University of Texas M. D. Anderson Cancer Center 1515 Holcombe Boulevard Houston, TX 77030 USA, Telephone: (713) 794-1769 Fax: (713) 792-7273 hamin@mdanderson.org.

Conflict of Interest statement

The authors declare no competing financial interests.

Introduction

The type I insulin-like growth factor receptor (IGF-IR) tyrosine kinase is composed of two identical α and two identical β subunits connected by disulfide bonds to form the functional transmembranous homodimeric protein complex [1,2]. Signaling through IGF-IR contributes to the establishment and progression of human malignancies. IGF-IR plays important roles in regulating cellular differentiation, shape, and migration, as well as metastatic dissemination [3–5]. The oncogenic potential of IGF-IR has been repeatedly documented in a large variety of solid tumors [6–11]. Notably, fewer studies have been performed to systematically explore the role of IGF-IR in hematologic neoplasms [12–20].

Picropodophyllin (PPP), an epimer of podophyllotoxin, appears to be particularly promising since it induces activation loop-specific inhibition of the tyrosine phosphorylation of IGF-IR without suppressing the activity of the insulin receptor or other more distantly related receptors [20,21]. Inhibition of IGF-IR tyrosine kinase with PPP does not interfere with ATP binding in the kinase domain, which suggests that it induces its inhibitory effect at the substrate level. PPP has demonstrated promising anti-tumor activity in several types of cancer, including plasma cell myeloma, medulloblastoma, ALK^+ anaplastic large-cell lymphoma, mantle cell lymphoma, chronic myeloid leukemia, and non-small cell lung cancer [13–16, 19–24]. Indeed, PPP (AXL1717) is currently used in Phase I/II clinical trials that include patients with some of the most aggressive and resistant types of cancer, and it appears to induce promising results with minimal side effects [24, http://clinicaltrials.gov/show/NCT01721577; http://clinicaltrials.gov/show/NCT01561456].

T lymphoblastic leukemia/lymphoma (T-LBL) is an aggressive hematological neoplasm [25]. Although it may occur any age group, T-LBL has the predilection to affect adolescents and young adults [26]. Typically, T-LBL presents with increased blasts in the bone marrow and peripheral blood. It often presents with large mediastinal mass, lymphadenopathy, and hepatosplenomegaly. Previous studies have shown that IGF-IR is overexpressed in T lymphoblasts [27, 28]. Importantly, a recent study has supported major contributions of IGF-IR to the survival of leukemia-initiating cells in T-LBL. This study also concluded that IGF-IR inhibitors could have a major impact on the treatment of this aggressive type of cancer in the near future [29]. Because PPP is a potent, selective inhibitor of IGF-IR that is currently being explored in clinical trials of resistant cancer patients with notable success, we set out to examine the effects of PPP on prototype T-LBL cell lines including Jurkat and Molt-3.

Materials and methods

Cell lines and treatments

Jurkat and Molt-3 cell lines (ATCC, Manassas, VA, USA) were maintained in RPMI 1640 supplemented with 10% FBS (Sigma), glutamine (2 mM), penicillin (100 U/ml), and streptomycin (100 μg/mL) at 37°C in humidified air supplemented with 5% CO_2. Selective targeting of IGF-IR was achieved by PPP (Calbiochem, Gibbstown, NJ, USA) after being dissolved in ethanol to a concentration of 0.5 mM (final concentration of ethanol was less than 0.4% by volume). PPP was added at the indicated concentrations in Jurkat and Molt-3

cells. In some experiments, Jurkat and Molt-3 cells were serum-deprived (1% FBS) for 16 h, treated with vehicle or PPP for 6 h, and then stimulated with human recombinant IGF-I (100 ng/mL; Peprotech. Rocky Hill, NJ, USA) for 15 min.

Cell viability, apoptosis, and cell cycle assays

Cell viability was evaluated by the Cell Counting Kit-8 (Dojindo, Tokyo, Japan) according to the manufacturer's instruction. Apoptosis was analyzed by flow cytometry (FACScalibur, BD Bioscenices, CA, USA) after staining the cells with annexin V-FITC and propidium iodide (PI) (Shanghai Majorbio Bio-Pharm Technology Co., China). Cell cycle analysis was performed using standard techniques. Briefly, cells were centrifuged for 5 min at 800 rpm and 4 °C, washed 2 times with PBS, and then suspended in 70% ethanol at 4°C overnight. Thereafter, cells were spun and resuspended in PBS that contained 50 μg/ml of PI and RNase A for 30 min at 37°C in the dark. The samples were analyzed by flow cytometery and the ModFit LT 2.0 software (Verity Software, Topsham, ME, USA).

Immunoprecipitation and Western blotting

Cell lysates were obtained using standard techniques and RIPA lysis buffer (Beyotime Institute of Biotechnology, Changzhou, China). For immunoprecipitation, lysates were incubated with IGF-IRβ (Zymed Laboratories, South San Francisco, CA, USA) antibody overnight at 4°C. Agarose beads conjugated with A/G were then added and incubated for 4 hours at 4°C. The immunocomplexes were spun, washed 3 times with cold phosphate buffered saline (PBS) and once with lysis buffer, and then subjected to sodium dodecyl sulfate–polyacrylamide gel electrophoresis (SDS-PAGE). For Western blotting (WB), proteins (50–80 μg) were electrophoresed on 6% to 12% SDS-PAGE then transferred to nitrocellulose membranes and probed with specific primary antibodies including IGF-IRβ (Zymed Laboratories, South San Francisco, CA, USA), pIGF-IR (Tyr1131), Phospho-Tyrosine, pAkt (Ser 473), Akt, pMAPK (Thr202/Tyr204), MAPK (Erk1/2), caspase-3, PARP (all from Cell Signaling Technology, Danvers, MA, USA), Bcl-2, cyclin B1, Bcl-X_L, p16, β-Actin, calreticulin thioredoxin reductase-1, and Ran-specific GTPase-activating protein (all from Epitomics, Burlingame, CA, USA). Thereafter, membranes were probed with the appropriate horseradish peroxidase-conjugated secondary antibodies (Sinbio, Shanghai, China). Bands were detected using chemiluminescence-based kit (GE Healthcare, Buckinghamshire, UK).

Protein sample preparation for proteomic analysis

Cell pellets were collected by centrifugation and washed 2 times with PBS, snap-frozen, and thereafter thawed in protein lysis buffer (8 M urea, 2% [w/v] CHAPS, 2% [v/v] carrier ampholyte, pH4–7, 40 mM DTT [dithiothreitol] and 0.002% [w/v] bromphenol blue). Insoluble materials were removed by centrifugation, the supernatant was collected, and protein content was determined by the Bradford method as previously described [30].

Two-dimensional polyacrylamide gel electrophoresis

200 μg proteins were loaded onto a 24-cm immobilized linear pH gradient (IPG) strip, pH 4–7 (GE Healthcare, Little Chalfont, Buckinghamshire, UK). Isoelectric focusing was

performed with the IPGphor system (GE Healthcare). For the second dimensional electrophoresis, SDS-polyacrylamide gel electrophoresis (PAGE) was performed on a vertical electrophoresis system (Ettan DALT6; GE Healthcare). Images of each gel were acquired using Lab-Scan version 3.0 software (GE Healthcare) and analyzed using ImageMaster 2DE platinum version 4.5 software (GE Healthcare). The experiments were repeated three times.

In-gel protein digestion, mass spectrometry analysis, and protein identification

Different proteins were excised from the two-dimensional gel and digested with trypsin, as previously described [31]. Mass spectra of the spots were acquired by 4800 Plus MALDI TOF/TOF™ Analyzer (Applied Biosystems, USA). Mass spectrometric data were analyzed using the matrix-Science Mascot bioinformatics database search engine for peptide mass fingerprint (PMF) matching against peptides from known protein sequences entered in publicly available UniProt databases (http://www.uniprot.org/uniprot/).

Statistical analysis

Experiments were performed in at least triplicates and repeated three times or more. The data are presented as means ± SD. Statistical analysis was performed by using Student t-test or one-way ANOVA test where appropriate. $P < 0.05$ was considered statistically significant.

Results

Inhibition of IGF-IR by PPP induces cell death in Jurkat cells

Inhibition of IGF-IR by PPP induced time- and concentration-dependent decrease in the viability of the T-LBL cells Jurkat and Molt-3 (Figure 1A). At 48 h after treatment, IC_{50} was 1.5 and 1.0 μM in Jurkat and Molt-3 cells, respectively (Figure 1A). Of important note is that we previously found that PPP does not decrease the viability of normal human T lymphocytes [15]. Furthermore, PPP induced concentration- and time-dependent increase in apoptotic cell death in Jurkat and Molt-3 cells (Figure 1B). Cells were considered apoptotic when stained for annexin V only or when stained simultaneously for annexin V and PI. In Jurkat and Molt-3 cells at 48 h of 2.0 uM PPP treatment, apoptosis was increased by 7.5 and 4.5-fold, respectively, compared to control untreated cells (Figure 1B). Cell cycle analysis revealed that PPP induced a G2/M-phase cell cycle arrest in both Jurkat and Molt-3 cells after 24 h and 48 h of treatment (Figure 1C).

PPP affects the levels of phosphorylated IGF-1R and downstream target molecules

We sought to explore a biochemical explanation for the PPP-induced death of Jurkat and Molt-3 cells. Western blotting and immunoprecipitation showed that PPP decreased the levels of tyrosine phosphorylated IGF-IR without altering baseline IGF-IR levels at 24 h (Figure 2A, 2B). A subsequent analyses of signal transduction pathways revealed that IGF-IR inhibition with PPP reduced activation of PI3K/Akt and MAPK/Erk signaling in Jurkat and Molt-3 cells (Figure 2A). PPP also caused downregulation of Bcl-2 and Bcl-$X_{L,}$ and induced activation of caspase-3 and PARP (Figure 2A), which is consistent with apoptotic cell death. Furthermore, inhibition of IGF-IR by PPP induced upregulation of cyclin B1.

However, changes were not seen in p16 (Figure 2A, 2B). Collectively, these results are consistent with G2/M-phase cell cycle arrest.

To examine whether the effects of PPP in T-LBL is mediated through inhibition of IGF-IR signaling, we first used IGF-I to stimulate serum-starved Jurakt and Molt-3. As demonstrated in Fig. 2C, PPP significantly decreased the tyrosine-phosphoryalted IGF-IR levels (Fig. 2C).

PPP changes expression of functional proteins

Proteins in Jurkat cells lysates were separated by 2-DE and the protein spots were visualized following Coomassie R-250 staining. Three pairs of gel from different batches of control and cells treated with 1.0 uM PPP for 24 h were analyzed for differential spot comparisons with the ImageMaster 2DE platinum version 4.5 software. Spots were compared based on volume percentage calculated as total spot volume to the whole gel image. Significantly changed spots were selected if there was at least 4-fold increase/decrease in their intensity. After the matching analysis, 7 protein spots were found to be significantly different in these two batches of gels, and they were picked out at the corresponding site (Fig. 3A). The proteins were identified by MALDI-TOF-MS on the basis of peptide mass matching following in-gel digestion with trypsin. The peptide masses were matched with the theoretical peptide masses of all proteins from the human species of the SwissProt database (Table 1). Figure 3B shows the spectrum of the trypsin digest of protein spot 1.

Five proteins were downregulated in PPP-treated cells including calreticulin, cytoplasmic actin-2, cytoplasmic thioredoxin reductase-1, Ran-specific GTPase-activating protein, and Rho GDP-dissociation inhibitor-2. In addition, two proteins were upregulated and identified as the UV excision repair protein RAD23 homolog B and tropomyosin beta chain. To validate the results obtained by the proteomic approach, we carried out Western blotting analysis with specific antibodies. WB confirmed the reduction in calreticulin, thioredoxin reductase-1, and Ran-specific GTPase-activating protein levels after treatment of Jurkat cells with PPP ($P < 0.05$) (Fig. 4A and 4B).

Discussion

Oncogenic signaling through the IGF-IR tyrosine kinase has become a major focus of cancer research. The important contribution of IGF-IR signaling to the survival of T-LBL has been recently documented [29]. In the present study, the significance of IGF-IR, as a potential molecular target in T-LBL, was stressed once again when PPP induced negative biological effects in Jurkat and Molt-3 cells. PPP is a cyclolignan that induces activation loop-specific inhibition of tyrosine phosphorylation of IGF-IR [22]. The effects of PPP in Jurkat and Molt-3 cells included down-regulation of PI3K/Akt and MAPK/Erk signaling pathways, which was associated with apoptosis and G2/M-phase cell cycle arrest, similar to previously reported effect of PPP in other type of cancer cells [13–16, 19]. It is important to emphasize that we have previously demonstrated that PPP failed to induce negative biological effects in 3 different types of normal human cells including skin fibroblasts, B lymphocytes, and T lymphocytes [15, 16, 19]. These findings are in agreement with the recently reported lack of significant untoward effects of some of the IGF-IR inhibitors, including PPP, that are

currently utilized in clinical trials of patients with solid tumors [22, 24, http://clinicaltrials.gov/show/NCT01721577, http://clinicaltrials.gov/show/NCT01561456]. Biochemical analysis of the effects of PPP in T-LBL showed activation of caspase-3 and PARP, downregulation of Bcl-2 and Bcl-X_L and upregulation of cyclin B1, which explain the occurrence of apoptosis and G2/M cell cycle arrest observed in these cells. Collectively, these findings further support important contributions of IGF-IR to the survival of T-LBL, and identify some of the possible mechanisms by which inhibition of IGF-IR with PPP induces negative biological effects in this type of cancer.

To our knowledge, this study is the first where proteomic analysis was used to analyze changes in protein expression induced by PPP, which is expected to expand current understanding of how PPP induces its effects in tumor cells. Our results showed that PPP induced significant downregulation of 5 proteins, including careticulin, in Jurakt cells. Calreticulin is a calcium-binding chaperone that plays versatile roles including folding, oligomeric assembly and quality control of related proteins in the ER via the calreticulin/calnexin cycle. This lectin interacts transiently with almost all of the monoglucosylated glycoproteins that are synthesized in the ER. Calreticulin also interacts with the DNA-binding domain of NR3C1 and mediates its nuclear export [32, 33]. The multiple activities of calreticulin suggest that its expression may be prevalent in many cellular compartments [34]. Our data indicate that PPP interferes with the expression of calreticulin and thus inhibit cancer cell growth.

Cytoplasmic actin-2 belongs to the actin family. Although actins are highly conserved proteins that are involved in various types of cell motility and are ubiquitously expressed in eukaryotic cells, individual actins perform distinct functions based on their polarized distributions in a variety of cells. Previous studies have shown that cytoplasmic actin-2 (cytoplasmic γ-actin) is not required for skeletal muscle development but its absence leads to a progressive myopathy and mutations in the γ-actin gene (ACTG1) are associated with dominant progressive deafness (DFNA20/26) [35, 36].

Cytoplasmic thioredoxin reductase 1 may possess glutaredoxin activity as well as thioredoxin reductase activity and induces actin and tubulin polymerization, leading to formation of cell membrane protrusions [37]. Ran-specific GTPase-activating protein (RanBP1), a small cytosolic protein, is a major regulator of the Ran GTPase that controls several cellular processes including nucleo-cytoplasmic transport, RNA processing, cell cycle progression, mitotic spindle formation, and post-mitotic nuclear assembly [38–40]. Elevated RanBP1 expression had been reported in a variety of human malignancies [41], and may be part of the regulatory mechanisms altered during tumourigenesis. Silencing of RanBP1 causes aberrant mitotic spindle formation, inhibition of cancer cell proliferation, and apoptosis [42, 43]. These observations, together with the findings of this study, suggest that the inhibition of proteins regulating microtubule dynamics and cell division may suppress tumor cell growth. Rho GDP-dissociation inhibitor 2 regulates the GDP/GTP exchange reaction of the Rho proteins by inhibiting the dissociation of GDP from them, and the subsequent binding of GTP to them [44, 45]. It acts as a negative regulator of Rho GTPases [46]. In addition, it controls subcellular localization of the Rho GTPases through binding the C-terminal isoprenoid modification, thus preventing their insertion into the

plasma membrane and modulating the ratio of the active membrane-bound and inactive soluble forms of Rho proteins [47]. Rho GDI was described as an antiapoptotic molecule that promotes the resistance of cancer cells to drug induced toxicity. Overexpression of Rho GDI in human breast cancer and lymphoma cells strongly inhibited apoptosis induced by two different chemotherapeutic agents: etoposide and doxorubicin [48]. Rho GDI was downregulated in response to chemotherapeutic drug treatments (all-trans retinoic acid and the cyclin-dependent kinase inhibitor bohemine) [49, 50]. Our results suggest that PPP treatment decreased the expression of Rho GDI, which might have contributed to enhancing T-LBL cellular apoptosis.

It is well known that PPP is a stereoisomer of podophyllotoxin (PPT), a potent tubulin inhibitor. Wu et al recently reported that, in human esophageal squamous cell carcinoma cell lines, the cytotoxicity and downregulation of pAkt observed after treatment with PPP result from microtubule inhibition (directly or indirectly through spontaneous PPT formation), rather than any effect of PPP on IGF-IR [51]. From our results, PPP efficiently blocked IGF-IR activity, reduced the phosphorylation of Akt (pAkt) and Erk1/2 (pErk1/2), induced apoptosis and G2/M cell cycle arrest in Jurkat and Molt-3 cells. Importantly, PPP also induced cell death in Jurkat and Molt-3 cells that were stimulated with IGF-I before treatment. These findings suggest that PPP inhibits IGF-I/IGF-IR signaling in T-LBL. However, similar to other small molecule inhibitors, we cannot completely exclude that PPP may induce inhibitory effects on other cellular survival molecules independent from its effects on IGF-IR. For instance, decreased levels of cytoplasmic thioredoxin reductase 1 after treating T-LBL cell lines with PPP suggests that PPP most likely interferes with tubulin polymerizationon. Further studies are required to further characterize the other candidates for PPP inhibitory effects on tumor cells growth and survival.

Upregulated proteins after treatment of Jurkat cells with PPP include the UV excision repair protein RAD23 homolog B and Tropomyosin beta chain, respectively. RAD23B is a multiubiquitin chain receptor involved in modulation of proteasomal degradation and may play a role in endoplasmatic reticulum-associated degradation (ERAD) of misfolded glycoproteins by association with PNGase and delivering deglycosylated proteins to the proteasome [52]. Elevated RAD23B expression suggests that PPP was involved in ubiquitin signaling pathway. Tropomyosin beta chain binds to actin filaments in muscle and non-muscle cells. It is implicated in stabilizing cytoskeleton actin filaments in non-muscle cells and may have a role in agonist-mediated receptor internalization [53]. It seems that the upregulation of Tropomyosin beta chain inhibits cancer cell growth. In short, these seven proteins are involved in various aspects of cellular metabolism, cytoskeleton organization, and signal transduction pathways.

In conclusion, we have shown that PPP induces significant alterations in several important signaling proteins in Jurkat cells and also inhibits fundamental pathways regulating cell survival in two T-LBL cell lines: Jurkat and Molt-3. Our data provide strong evidence that targeting IGF-IR by PPP represents a potential therapeutic modality that can be successfully utilized to eradicate the aggressive T-LBL.

Acknowledgments

This work was sponsored by grants from National Natural Science Foundation of China (31100549), Shanghai Pujiang Programs (10PJ1402300 & 11PJ1400100), Innovation Program of Shanghai Municipal Education Commission (11ZZ51), the Scientific Research Foundation for the Returned Overseas Chinese Scholars, State Education Ministry and Fundamental Research Funds for the Central Universities (WF1114020 & 222201313010). HMA is supported by R01 CA151533 grant from the National Cancer Institute.

References

1. Ullrich A, Gray A, Tam AW, et al. Insulin-like growth factor I receptor primary structure: comparison with insulin receptor suggests structural determinants that define functional specificity. EMBO J. 1986; 5:2503–2512. [PubMed: 2877871]
2. De Meyts P, Whittaker J. Structural biology of insulin and IGF1 receptors: implications for drug design. Nat Rev Drug Discov. 2002; 1:769–783. [PubMed: 12360255]
3. Lopez T, Hanahan D. Elevated levels of the IGF-I receptor convey invasion and metastatic capability in a mouse model of pancreatic islet tumourigenesis. Cancer Cell. 2002; 1:339–353. [PubMed: 12086849]
4. Mauro L, Bartucci M, Morelli C, Ando S, Surmacz E. IGF-I receptor-induced cell-cell adhesion of MCF-7 breast cancer cells requires the expression of junction protein ZO-1. J Biol Chem. 2001; 276:39892–39897. [PubMed: 11518717]
5. Van Golen CM, Schwab TS, Kim B, et al. Insulin-like growth factor-I receptor expression regulates neuroblastoma metastasis to bone. Cancer Res. 2006; 66:6570–6578. [PubMed: 16818629]
6. Adachi Y, Lee CT, Coffee K, et al. Effects of genetic blockade of the insulin-like growth factor receptor in human colon cancer cell lines. Gastroenterology. 2002; 123:1191–1204. [PubMed: 12360481]
7. Burfeind P, Chernicky CL, Rininsland F, Ilan J. Antisense RNA to the type I insulin-like growth factor receptor suppresses tumor growth and prevents invasion by rat prostate cancer cells in vivo. Proc Natl Acad Sci USA. 1996; 93:7263–7268. [PubMed: 8692980]
8. Dunn SE, Ehrlich M, Sharp NJ, et al. A dominant negative mutant of the insulin-like growth factor-I receptor inhibits the adhesion, invasion, and metastasis of breast cancer. Cancer Res. 1998; 58:3353–3361. [PubMed: 9699666]
9. Hongo A, Kuramoto H, Nakamura Y, et al. Antitumor effects of a soluble insulin-like growth factor I receptor in human ovarian cancer cells: advantage of recombinant protein administration in vivo. Cancer Res. 2003; 63:7834–7839. [PubMed: 14633710]
10. Lee CT, Park KH, Adachi Y, et al. Recombinant adenoviruses expressing dominant negative insulin-like growth factor-I receptor demonstrate antitumor effects on lung cancer. Cancer Gene Ther. 2003; 10:57–63. [PubMed: 12489029]
11. Yin S, Girnita A, Stromberg T, et al. Targeting the insulin-like growth factor-1 receptor by picropodophyllin as a treatment option for glioblastoma. Neuro Oncol. 2010; 12:19–27. [PubMed: 20150364]
12. Bertrand FE, Steelman LS, Chappell WH, et al. Synergy between an IGF-1R antibody and Raf/MEK/ERK and PI3K/Akt/mTOR pathway inhibitors in suppressing IGF-1R mediated growth in hematopoietic cells. Leukemia. 2006; 20:1254–1260. [PubMed: 16642049]
13. Strömberg T, Ekman S, Girnita L, et al. IGF-1 receptor tyrosine kinase inhibition by the cyclolignan PPP induces G2/M-phase accumulation and apoptosis in multiple myeloma cells. Blood. 2006; 107:669–678. [PubMed: 16166596]
14. Menu E, Jernberg-Wiklund H, Strömberg T, et al. Inhibiting the IGF-1 receptor tyrosine kinase with the cyclolignan PPP: an in vitro and in vivo study in the 5T33MM mouse model. Blood. 2006; 107:655–660. [PubMed: 16046527]
15. Shi P, Lai R, Lin Q, et al. IGF-IR tyrosine kinase interacts with NPM-ALK oncogene to induce survival of T-cell ALK^{+} anaplastic large-cell lymphoma cells. Blood. 2009; 114:360–370. [PubMed: 19423729]

16. Shi P, Chandra J, Sun X, et al. Inhibition of IGF-IR tyrosine kinase induces apoptosis and cell cycle arrest in imatinib-resistant chronic myeloid leukemia cells. J Cell Mol Med. 2010; 14:1777–1792. [PubMed: 19508387]
17. Tazzari PL, Tabellini G, Bortul R, et al. The insulin like growth factor-I receptor kinase inhibitor NVP-AEW541 induces apoptosis in acute myeloid leukemia cells exhibiting autocrine insulin-like growth factor-I secretion. Leukemia. 2007; 21:886–896. [PubMed: 17361225]
18. Wahner Hendrickson AE, Haluska P, Schneider PA, et al. Expression of insulin receptor isoform A and insulin-like growth factor-1 receptor in human acute myelogenous leukemia: effect of the dual-receptor inhibitor BMS-536924 in vitro. Cancer Res. 2009; 69:7635–7643. [PubMed: 19789352]
19. Vishwamitra D, Shi P, Wilson D, et al. Expression and effects of inhibition of IGF-IR tyrosine kinase in mantle cell lymphoma. Haematol. 2011; 96:871–880.
20. Shi B, Vishwamitra D, Granda JG, Whitton T, Shi P, Amin HM. Molecular and functional characterizations of the association and interactions between nucleophosmin-anaplastic lymphoma kinase and type I insulin-like growth factor receptor. Neoplasia. 2013; 15:669–683. [PubMed: 23730215]
21. Girnita A, Girnita L, Del Prete F, Bartolazzi A, Larsson O, Axelson M. Cyclolignans as inhibitors of the insulin-like growth factor-1 receptor and malignant cell growth. Cancer Res. 2004; 64:236–242. [PubMed: 14729630]
22. Vasilcanu D, Girnita A, Girnita L, Vasilcanu R, Axelson M, Larsson O. The cyclolignan PPP induces activation loop-specific inhibition of tyrosine phosphorylation of the insulin-like growth factor-1 receptor. Link to phosphatidyl inositol-3 kinase/Akt apoptotic pathway. Oncogene. 2004; 23:7854–7862. [PubMed: 15334055]
23. Ohshima-Hosoyama S, Hosoyama T, Nelon LD, Keller C. IGF-1 receptor inhibition by picropodophyllin in medulloblastoma. Biochem Bioph Res Commun. 2010; 399:727–732.
24. Ekman S, Frödin J, Harmenberg J, et al. Clinical Phase I study with an Insulin-like Growth Factor-1 Receptor Inhibitor: Experiences in patients with squamous non-small cell lung carcinoma. Acta Oncol. 2011; 50:441–447. [PubMed: 20698809]
25. Thomas DA, Kantarjian HM. Lymphoblastic lymphoma. Hematol/Oncol Clin North Am. 2001; 15:51–95.
26. Borowitz, MJ.; Chan, JKC. T lymphoblastic leukemia/lymphoma. In: Swerdlow, SH.; Campo, E.; Harris, NL., et al., editors. WHO classification of tumours of haematopoietic and lymphoid tissues. IARC; Lyon: 2008. p. 176-178.
27. Lee PD, Rosenfeld RG, Hintz RL, Smith SD. Characterization of insulin, insulin-like growth factors I and II, and growth hormone receptors on human leukemic lymphoblasts. J Clin Endocrinol Metab. 1986; 62:28–35. [PubMed: 2999181]
28. Baier TG, Ludwig WD, Schönberg D. KKPHartmann, Characterisation of insulin-like growth factor I receptors of human acute lymphoblastic leukaemia (ALL) cell lines and primary ALL cells. Eur J Cancer. 1992; 28A:1105–1110. [PubMed: 1378290]
29. Medyouf H, Gusscott S, Wang H, et al. High-level IGF1R expression is required for leukemia-initiating cell activity in T-ALL and is supported by Notch signaling. J Exp Med. 2011; 208:1809–1822. [PubMed: 21807868]
30. Bradford MM. A rapid and sensitive method for the quantitation of microgram quantities of protein utilizing the principle of protein-dye binding. Anal Biochem. 1976; 72:248–254. [PubMed: 942051]
31. Bergman AC, Benjamin T, Alaiya A, et al. Identification of gel separated tumor marker proteins by mass spectrometry. Electrophoresis. 2000; 21:679–686. [PubMed: 10726777]
32. Nauseef WM, McCormick SJ, Clark RA. Calreticulin functions as a molecular chaperone in the biosynthesis of myeloperoxidase. J Biol Chem. 1995; 270:4741–4747. [PubMed: 7876246]
33. Holaska JM, Black BE, Love DC, Hanover JA, Leszyk J, Paschal BM. Calreticulin is a receptor for nuclear export. J Cell Biol. 2001; 152:127–140. [PubMed: 11149926]
34. Tarr JM, Young PJ, Morse R, et al. A mechanism of release of calreticulin from cells during apoptosis. J Mol Biol. 2010; 401:799–812. [PubMed: 20624402]

35. Van Wijk E, Krieger E, Kemperman MH, et al. A mutation in the gamma actin 1 (ACTG1) gene causes autosomal dominant hearing loss (DFNA20/26). J Med Genet. 2003; 40:879–884. [PubMed: 14684684]
36. Sonnemann KJ, Fitzsimons DP, Patel JR, et al. Cytoplasmic γ-actin is not required for skeletal muscle development but its absence leads to a progressive myopathy. Dev Cell. 2006; 11:387–397. [PubMed: 16950128]
37. Dammeyer P, Damdimopoulos AE, Nordman T, Jimenez A, Miranda-Vizuete A, Arner ESJ. Induction of cell membrane protrusions by the N-terminal glutaredoxin domain of a rare splice variant of human thioredoxin reductase 1. J Biol Chem. 2008; 283:2814–2821. [PubMed: 18042542]
38. Bischoff FR, Krebber H, Kempf T, Hermes I, Ponsting H. Human Ran GTPase-activating protein RanGAP1 is a homologue of yeast Rna1p involved in mRNA processing and transport. Proc Natl Acad Sci USA. 1995; 92:1749–1753. [PubMed: 7878053]
39. Kalab P, Pu RT, Dasso M. The ran GTPase regulates mitotic spindle assembly. Curr Biol. 1999; 9:481–484. [PubMed: 10322113]
40. Nishimoto T. A new role of ran GTPase. Biochem Biophys Res Commun. 1999; 262:571–574. [PubMed: 10471364]
41. Antonucci F, Chilosi M, Parolini C, Hamdan M, Astner H, Righetti PG. Two-dimensional molecular profiling of mantle cell lymphoma. Electrophoresis. 2003; 24:2376–2385. [PubMed: 12874873]
42. Jeha S, Luo XN, Beran M, Kantarjian H, Atweh GF. Antisense RNA inhibition of phosphoprotein p18 expression abrogates the transformed phenotype of leukemic cells. Cancer Res. 1996; 56:1445–1450. [PubMed: 8640838]
43. Gez S, Crossett B, Christopherson RI. Differentially expressed cytosolic proteins in human leukemia and lymphoma cell lines correlate with lineages and functions. Biochim Biophys Acta. 2007; 1774:1173–1183. [PubMed: 17698427]
44. Scherle P, Behrens T, Staudt LM. Ly-GDI, a GDP-dissociation inhibitor of the RhoA GTP-binding protein, is expressed preferentially in lymphocytes. Proc Natl Acad Sci USA. 1993; 90:7568–7572. [PubMed: 8356058]
45. Scheffzek K, Stephan I, Jensen ON, Illenberger D, Gierschik P. The Rac-RhoGDI complex and the structural basis for the regulation of Rho proteins by RhoGDI. Nat Struct Bio. 2000; 7:22–126. [PubMed: 10625421]
46. Olofsson B. Rho guanine dissociation inhibitors: pivotal molecules in cellular signaling. Cell Signal. 1999; 11:545–554. [PubMed: 10433515]
47. Bilodeau D, Lamy S, Desrosiers RR, Gingras D, Beliveau R. Regulation of Rho protein binding to membranes by rhoGDI: inhibition of releasing activity by physiological ionic conditions. Biochem Cell Biol. 1999; 77:59–69. [PubMed: 10426287]
48. Zhang B, Zhang Y, Dagher MC, Shacter E. Rho GDP dissociation inhibitor protects cancer cells against drug-induced apoptosis. Cancer Res. 2005; 65:6054–6062. [PubMed: 16024605]
49. Kovarova H, Hajduch M, Korinkova G, et al. Proteomics approach in classifying the biochemical basis of the anticancer activity of the new olomoucine-derived synthetic cyclin-dependent kinase inhibitor, bohemine. Electrophoresis. 2000; 21:3757–3764. [PubMed: 11271495]
50. Wan J, Wang J, Cheng H, et al. Proteomic analysis of apoptosis initiation induced by all-trans retinoic acid in human acute promyelocytic leukemia cells. Electrophoresis. 2001; 22:3026–3037. [PubMed: 11565797]
51. Wu X, Sooman L, Wickström M, Fryknäs M, Dyrager C, Lennartsson J, Gullbo J. Alternative cytotoxic effects of the postulated IGF-IR inhibitor picropodophyllin in Vitro. Mol Cancer Ther. 2013; 12:1526–1536. [PubMed: 23699657]
52. Dantuma NP, Heinen C, Hoogstraten D. The ubiquitin receptor Rad23: at the crossroads of nucleotide excision repair and proteasomal degradation. DNA Repair (Amst). 2009; 8:449–460. [PubMed: 19223247]
53. Libri D, Mouly V, Lemonnier M, Fiszman MY. A nonmuscle tropomyosin is encoded by the smooth/skeletal beta-tropomyosin gene and its RNA is transcribed from an internal promoter. J Biol Chem. 1990; 265:3471–3473. [PubMed: 2303454]

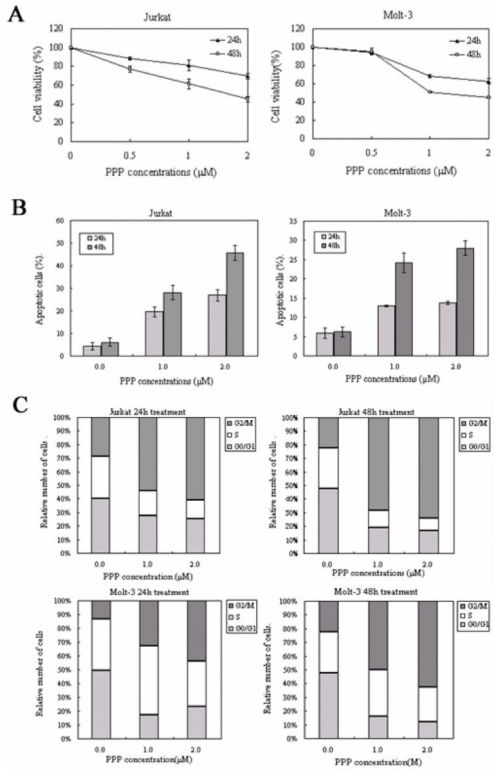

Figure 1.

PPP induces negative biologic effects in Jurkat and Molt-3 cells. (A) PPP induces a concentration- and time-dependent decrease in Jurkat and Molt-3 cell viabilities. (B) PPP also induces a concentration- and time-dependent increase in apoptotic cell death of Jurkat and Molt-3 cells. All treatments were statistically significant compared with control untreated cells ($P<0.05$). (C) Treating Jurkat and Molt-3 cells with PPP induces G2/M-phase cell-cycle arrest. Data are shown as means ± SD of three separate experiments.

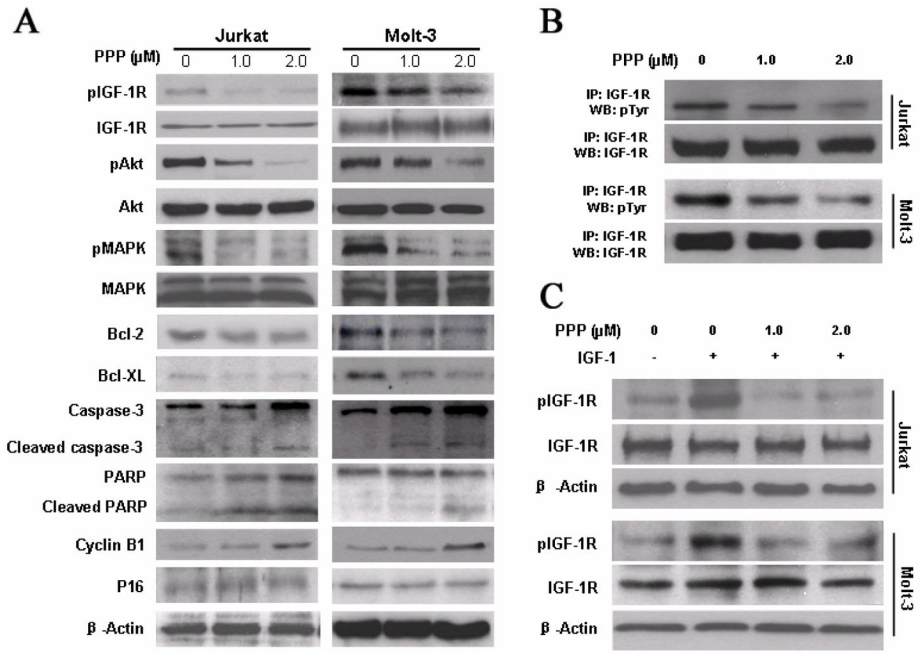

Figure 2.

PPP induces significant effects on downstream target proteins of IGF-IR in Jurkat and Molt-3 cells. (A) Western blotting confirmed that at 24 hours, PPP induces marked down-regulation of pIGF-IR, without a noticeable change in IGF-IR levels. In addition, PPP induces significant activation of Caspase-3 and PARP, and decreases in the levels of the antiapoptotic proteins Bcl-2 and Bcl-X_L. Furthermore, PPP induces a notable increase in the cell-cycle regulatory protein cyclin B1. Changes are not seen in p16. β-actin was used as an internal control. Each experiment was repeated three times with similar results. (B) Immunoprecipitation showed that PPP induces significant down-regulation of pIGF-IR, without a noticeable change in IGF-IR levels. Representative results were shown (n=3). (C) The stimulation with IGF-1 showed that obvious down-regulation of pIGF-IR and PPP efficiently blocks IGF-IR activity and, pIGF-IR was down-regulated. β-actin was used as an internal control. Each experiment was repeated three times with similar results.

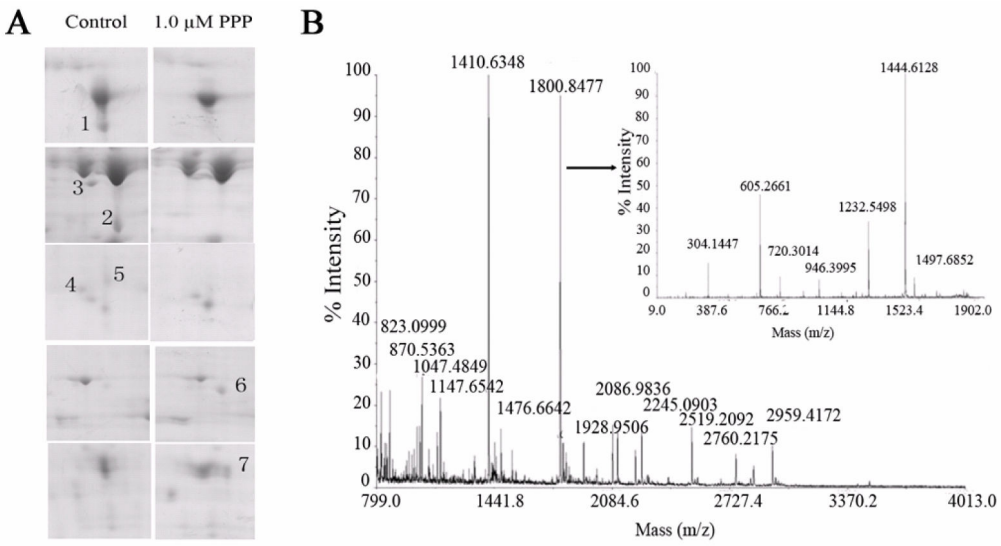

Figure 3.

PPP affects the proteins expression in Jurkat cells. (A) Partial maps of the two-dimensional electrophoresis analysis of total proteins in Jurkat cells. Digits represent the differential spots. Spots 1–5 are the downregulated proteins and spots 6–7 are the upregulated ones. (B) Peptide mass fingerprint of protein spot 1 excised from the two-dimensional electrophoresis gel.

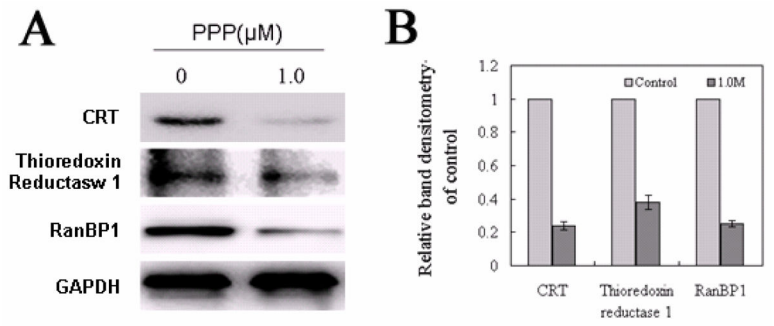

Figure 4.

PPP induces downregulation of calreticulin, thioredoxin reductase-1 and Ran-specific GTPase-activating protein. (A) Western blotting shows that PPP induces significant downregulation of calreticulin, thioredoxin reductase-1 and Ran-specific GTPase-activating protein levels. GAPDH was used as internal control. (B) Histograms represent relative WB band densitometry of control, compared to the corresponding band densitometry of GAPDH. Data are shown as means ± SD of three separate experiments.

Table 1

Proteins identified by using peptide mass fingerprint data from matrix-assisted laser desorption/ionization time-of-flight mass spectrometry (MALDI-TOF-MS) and searching the protein databases (http://www.uniprot.org/uniprot/ and http://www.hprd.org/).

Spot	Protein Score	Peptide matches	AC	ID	pI	Mr Dalton	Function
1	597	19	P27797	Calreticulin	4.29	48282.9	Protein metabolism
2	551	13	P63261	actin, cytoplasmic 2	5.31	42107.9	Cell growth and/or maintenance
3	271	17	Q16881	Thioredoxin reductase 1, cytoplasmic	6.02	55470.2	Metabolism; Energy pathways
4	211	10	P43487	Ran-specific GTPase-activating protein	5.19	23466.6	Cell communication; Signal transduction
5	265	12	P52566	Rho GDP-dissociation inhibitor 2	5.1	23030.6	Cell communication; Signal transduction
6	258	11	P54727	UV excision repair protein RAD23 homolog B	4.79	43201.6	Regulation of nucleobase, nucleoside, nucleotide and nucleic acid metabolism
7	200	16	P07951	Tropomyosin beta chain	4.63	33026.6	Cell growth and/or maintenance